ELSEVIER

Chemical Engineering Journal 81 (2001) 251–260

Chemical Engineering Journal

www.elsevier.com/locate/cej

Gamma ray tomography design for the measurement of hold-up profiles in two-phase bubble columns

U. Parasu Veera*

Department of Chemical Technology, Chemical Engineering Division, University of Mumbai, Matunga, Mumbai-400 019, India

Received 25 October 1999; received in revised form 26 April 2000; accepted 1 May 2000

Abstract

A gamma ray tomography system was designed, developed and employed for the measurement of radial hold-up profiles in bubble columns. Measurements were of gamma ray attenuation. For the given source strength the collimator designs for both source and detectors were optimized to get the maximum number of counts with the least scattering effects. For the given dwell and scanning times, excellent reproducibility was obtained. Both fan beam and pencil beam scanning were employed to minimize the error due to scattering of the photons near to the wall regions. Experiments were performed in a 0.385 m internal diameter bubble column. Chordal hold-up profiles were used to find the radial hold-up profile using Abel's inversion method.

Keywords: Tomography; Chordal and radial hold-up profiles; Bubble column

1. Introduction

Bubble columns are extensively used in the chemical and biochemical industries. The flow of gas phase in bubble column can be broadly divided into two regimes: homogeneous and heterogeneous. In the homogeneous regime the gas bubbles rise without any significant coalescence or breakage. The size of bubbles is uniform and the hold-up profile is practically flat in the transverse direction. The heterogeneous regime is characterized by non-uniformity of the bubble shape and size, and a hold-up profile with intense liquid circulation. The average gas hold-up is a global parameter and it is useful in deciding the size of the reactor. The radial hold-up profiles, which give local gas concentration, help in understanding the flow pattern.

Measurement of radial hold-up profiles in two-phase flow was first reported by Neal and Bankoff [1]. Since then many groups have reported such measurements using different techniques, such as conductivity probe, electro-resistivity probe, optical probe, hot-film anemometer, particle image velocimetry (PIV), ultrasonic techniques, electrical capacitance and resistance tomography and gamma ray tomography. Joshi et al. [2] reviewed these techniques extensively. The gamma ray tomography technique is non-intrusive and it does not disturb the flow.

Measurement of gas hold-up profiles using electrical properties (conductivity probe, electro resistivity probe) can be done only if the liquid phase is conductive. The transient responses of these probes are relatively slow and the probes disturb the flow (Begovich and Watson [3], Achwal and Stepanek [4]). Thermal anemometers are also widely used for local measurement, using the principle of detection of change in the heat transfer rate from a small, electrically heated sensor and the fluid. This heat transfer rate depends on the fluid velocity, the temperature difference between sensor and fluid, physical properties of the fluid and the dimensions and physical properties of the sensor (Delhaye et al. [5]). The measurement becomes very difficult if all the above parameters vary, leading to inaccurate measurements. The radiation-based measurements have replaced these conventional measurements, as they are non-intrusive and non-destructive. X-ray imaging and the neutron scattering techniques have not received wide acceptance, as the generation of X-rays is tedious, beam intensity can fluctuate and X-ray's have low penetration through metal test sections. On the other hand neutron scattering measurements need long measuring times, as the intensity of the scattering beam is very small. All these limitations are practically eliminated by the gamma ray attenuation technique. Bennet et al. [6] used the electrical capacitance tomography (ECT) technique for the measurement of gas concentration in two-phase bubble columns with an electrode array. Differences in capacitance properties are utilized in applying this technique for air and double distilled water system.

* Present address: IPP-CT, University of Twente, PB 217, 7500 AE, Enschede, The Netherlands. Tel.: +31-53-489-3030; fax: +31-53-489-4738.
E-mail address: u.parasuveera@ct.utwente.nl (U. Parasu Veera).

1385-8947/01/$ – see front matter
PII: S1385-8947(00)00202-3

Nomenclature

A	attenuation
Ac	activity of the source
c_{mn}	inverse Abel transform coefficient
d_{mn}	forward Abel transform coefficient
d	equivalent diameter of the beam
D_d	detector aperture, mm
e	emission ratio
f	detector efficiency
G	geometric factor ($T\Omega$)
I	intensity of the gamma rays (counts)
r	radial distance from the center of the column
R	radius of the column
S	sensitivity
t	path length
T	transmission (I/I_O)
X_d	distance of the scattering event from the detector
Z	distance between the source and detector

Greek letters

ε_{chord}	chordal hold-up
$\bar{\varepsilon}_G$	average gas hold-up
Ω	geometry factor as defined in Eq. (4)
μ	attenuation coefficient
ϕ	statistical error

Subscripts

G	gas
L	liquid
TP	two phase
O	incident ray

On similar principle, electrical impedance/resistance tomography techniques developed were reported by Wang et al. [7]. In electrical-tomography techniques, the field projected between source and detector does suffer deformation, making reconstruction difficult. In radiation based tomography techniques, beam does not suffer the deformation (Bennet et al. [6]). Ultrasound computerized tomography (UCT) has been studied since the early 1980 by several research groups. Xu et al. [8] used UCT in transmission mode to analyze the gas–liquid flow. Wiegand and Hoyle [9] used UCT in reflection mode to analyze the two-phase flow. Many difficulties have been addressed in ultrasound techniques, such as complex sound field sensed by transducers, which could result in overlapped or multiple reflected pulses (Li and Hoyle [10]).

Gamma ray tomography technique can also be extended to gas–solid and gas–liquid–solid systems with minor mathematical manipulations with certain assumptions. Bukur et al. [11] reported results for three-phase system. In the present paper, a systematic and simple design procedure for gamma ray tomography was presented for two-phase bubble column reactors.

2. Design procedure

In the design of a gamma ray tomography system the important parameters [12] to be considered are

- geometry of the test section and material of construction;
- selection of gamma source that is suitable for the test section together with its contents;
- estimation of the required source strength for the given experimental conditions;
- selection of scintillators;
- design of source and detector collimators;
- nuclear instrumentation and its compatibility for the present generation computers.

2.1. Test section

For the proper design of tomography system, test section dimensions and material of construction are important factors. The test section used determines the photon energy and the source strength required. In general, the source should have monoenergetic gamma rays and with an energy capable of penetrating through the test section with acceptable attenuation. At the same time the energy should be low enough to be sensitive to the contents. That requires either a low source strength of a high-energy gamma source or a high source strength of a low-energy gamma source for the required sensitivity of the source for the test section contents. The ratio of the attenuated intensity to the incident gamma ray intensity (I/I_O) is called transmission. Since the attenuation by the test section walls is constant (for a given section), transmission through the test section contents can be obtained by ratio of intensity of the empty section to the intensity of the source through the filled section. For good sensitivity, a low ratio is desired.

2.2. Selection of the gamma source

Transmission through the test-section walls and sensitivity to the test-section contents are major factors for the selection of the gamma source. The other constraints include, half-life, emission ratio, cost and availability. The emission ratio is defined as the number of photons of particular energy emitted per 100 disintegrations of the radionuclide. The lower the emission ratio, higher the source strength required for the desired count rate. This increases the handling problems and safety requirements and therefore, a high emission ratio is desired. The source used in the present investigation is ^{137}Cs that has an emission ration of 85.2%, although ^{60}Co has got highest emission ratio (99.98%). The reason for this is the half-life of the ^{137}Cs is 30.1 years whereas for ^{60}Co it is only 5.27 years. This reduces the procurement cost of the gamma source enormously. The Cs-137 source

gives out 85.2 of 662 keV energy photons out of 100 photons disintegrated from the Cs nucleus. When a source gives out photons of different energies, a monoenergetic beam can be detected by adjusting the window energy of a single channel analyzer in its count mode. This is discussed in detail later under the section of the single channel analyzer.

2.3. Source strength

The source strength required depends on, the count rate, beam size, losses through the test section walls, etc., collimator distance, scintillator efficiency and emission ratio of the gamma source. The calculation of source strength also depends on the maximum acceptable measurement error. With the tomography system operating in count mode, the errors involved are, geometry (curvature), flow-regime related errors and statistical errors. Statistical error only determines the source strength. For a give count rate, the statistical error is given by

$$\phi = \frac{\sqrt{I}}{I} = \frac{1}{\sqrt{I}} \tag{1}$$

where I is the number of counts for a long averaged period of time. Let I and I_O are the intensities of the gamma rays through the test section when full and when empty, respectively. Then the sensitivity (S) of the gamma rays to the contents of the test section can be defined as

$$S = \frac{I_O - I}{(I + I_O)/2} = \frac{2(1-T)}{(1+T)} \tag{2}$$

where $T{=}I/I_O$ is called transmission. It is clear that the statistical error is inversely proportional to the sensitivity. For a given count rate, higher the sensitivity, smaller the error will be. This is one of the main reasons why the use of lower energy gamma is desirable. Sensitivity, S, can be readily fixed by calculating the transmission for the given test section and for the given source. So the required source strength in disintegrations per second can be calculated for the required count rate (I_R) as

$$\mathrm{Ac} = \frac{I_R}{(Gfe)} \tag{3}$$

where G is a geometric factor, which takes into account the beam size, collimator distance and other transmission losses, f the efficiency of the scintillator used and e the source emission ratio. The geometric factor, G, is defined as the product of the transmission ratio, T and solid angle factor Ω defines as

$$\Omega = \frac{1}{4(d/Z)^2} \tag{4}$$

where d is the equivalent diameter of the beam having same area of sphere of that detector collimator area and Z the distance between source and detector.

Table 1
Some inorganic scintillator crystal properties

Scintillator	Decay constant (μs)	Density (gm/cm^3)	Conversion efficiency (%)
NaI (Tl)	0.23	3.67	100
CsI (Na)	0.63	4.51	85
CsI (Tl)	1.0	4.51	45
CsF	0.005	4.11	3
^{6}LiI (Eu)	1.4	4.08	35
CaF_2 (Eu)	0.9	3.19	50
BaF_2	0.63	4.88	10
KI (Tl)	0.24/0.25	3.13	24
Ps	∼0.002	1.05	<5

2.4. Selection of scintillators

Another important step in gamma ray tomography system design is the selection of scintillation detectors. Two parameters are important while selecting the scintillation detectors: detection efficiency and decay constant of the scintillator. High detection efficiency is required to reduce the source strength and short decay constant is required for high count rate to avoid pulse pileup or saturation, if the system is operated in count mode. NaI (Tl) crystal is most commonly used scintillator for its highest detection efficiency. Various scintillator properties are tabulated in Table 1.

2.5. The design of source and detector collimators

In the present investigation the disc source of ^{137}Cs was used. The disc source is a sealed source of 2 cm in diameter. The source was collimated in a lead brick with a central slit of 35 mm×8 mm×30 mm which provides a fan beam subtending an angle of 30° in the horizontal plane.

The photon emerging from the source interacts with the medium through which it passes and part of its energy is transferred to the electron. This gamma ray photon deflects through an angle with respect to its original direction. A collimator is used at the detector end to minimize the detection of the low energy scattered photons. Swift et al. [13] have derived the following expression for the measured transmission ratio accounting for the effects of forward scattering of the photons:

$$\frac{I}{I_O} = \mathrm{e}^{-\mu t} + 0.5\left(\frac{D_d}{X_d}\right)^2 (1 - \mathrm{e}^{-\mu t}) \tag{5}$$

The second term on the right-hand side of the above equation accounts for the scattering effects. D_d and X_d are the detector aperture and the distance of the scattering event from the detector.

2.6. Nuclear instrumentation

Nuclear instrumentation or counting systems are classified into two types according to the method of operation as

- pulse-type system;
- current-type system.

2.6.1. Pulse-type systems

In case of a pulse-type system, the output consists of voltage pulses and one pulse per particle is detected. It consists of instruments (modules) including a detector, multi-counter unit of multi-channel nuclear counting system consisting of high voltage supply for detectors, associated amplifiers and single channel analyzer for each channel and a data acquisition system.

2.6.1.1. Detector. The function of the detector is to produce a signal for every particle entering in it. Every detector works with a principle of interaction of particle with matter. Scintillation detectors are commonly used in most applications. In the present work, a scintillation detector is used for the detection of gamma radiation.

2.6.1.2. Scintillation detectors. A scintillation detector is a unit, which is used for the detection of gamma radiation. It consists of a scintillator and a photo multiplier tube (PMT). Scintillators are materials — solids, liquids, gases — that produce sparks or scintillators of light when ionizing radiation passes through them. The amount of light produced in the scintillator is very small and hence it must be amplified before it can be recorded as a pulse. A photomultiplier tube is used for the amplification or multiplication of the light emitted by scintillator.

Inorganic and organic scintillators are commonly used for scintillator detectors. Inorganic scintillators, however, are found to be superior to organic scintillators as respective response times are 10 ns and 1 μs. Inorganic scintillators respond much more quickly.

NaI (Tl) is the most commonly used inorganic scintillator for gamma rays. It has relatively high density ($3.67\times10^3\,kg/m^3$) and high atomic number, which makes it extremely efficient gamma detector. Its light conversion efficiency is the highest of all the inorganic scintillators (100%).

2.6.1.3. The photomultiplier tube (PMT). The photo multiplier tube or photo tube is an integral part of a scintillation counter. Without the amplification produced by the PMT, a scintillator is not useful for radiation detection. A PMT is essentially a fast multiplier that amplifies an incident pulse of visible light by a factor of 10^6 or more in times of 10^{-9} s. A photo-tube consists of an evacuated glass tube with photocathode at its center and several dynodes in the interior (Fig. 1). The photons produced in the scintillator enter the photo tube and hit the photo cathode, which is made of material (Cs–Sb compounds is used as photocathode in most of the scintillation detectors because its surface has maximum sensitivity for electron emission) that emit electrons when light strikes it. The electron emitted by the photocathode is guided with an electric field towards the first dynode, which is coated with a substance that emits secondary electrons, if an electron strikes it. The secondary emission rate depends on applied voltage and on the type of surface. The secondary

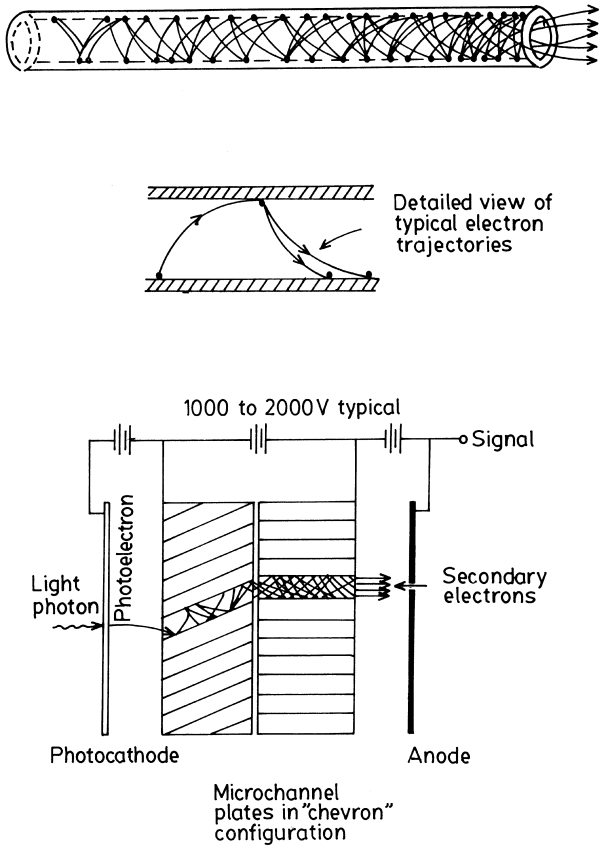

Fig. 1. Schematic diagram of the interior of a photomultiplier tube.

electrons from the first dynode move towards the second, from there towards the third and so on. The acceleration of electrons from one dynode to another is achieved by applying a successively increasing positive high voltage to each dynode. The voltage different between two successive dynodes is of the order of 80–120 V. Typical commercial photo tubes (Fig. 2, Khare [14]) may have up to 15 dynodes and the detectors used in the present investigation have 11 dynodes.

2.6.1.4. The amplifier. The main purpose of the amplifier is to amplify the signal that comes out of the detector. The signal that comes from the detector is very weak, i.e. of mV range. Before it can be recorded, it should be amplified by a factor of thousand or more which is done by the amplifier. In short, the amplifier increases the amplitude of pulse from detectors to a few volts as required by the analyzer that follows the amplifier with the provision for a gain selection and pulse shaping time constant.

2.6.1.5. The single channel analyzer. This is the most important unit in the gamma ray spectrometer and does the job of amplitude selection (and hence energy selection) for output pulses from the amplifier. Analyzers have base line and window setting selection or lower discriminator and upper discriminator level selections, typically denoted as E and ΔE, respectively. There is also a provision for threshold

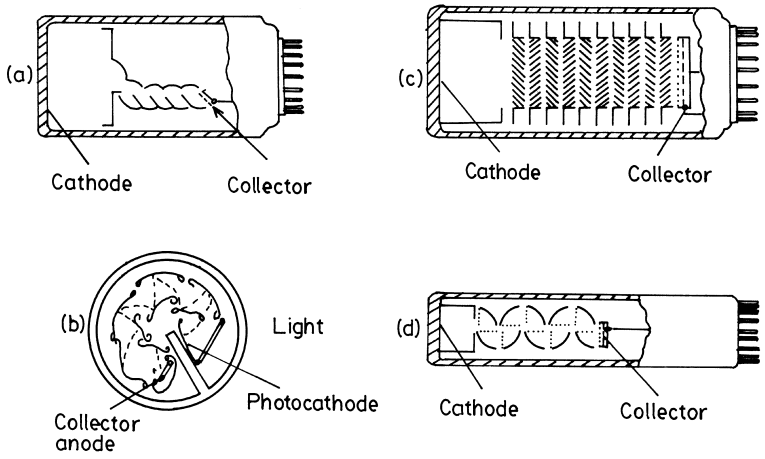

Fig. 2. Configurations of commercial photo multiplier tubes.

and window counting mode. In the threshold mode only the lower level discriminator or E operates. In the window mode position both E and ΔE, i.e. lower and upper level discriminators operate. The photons with energy above a certain threshold energy (E) and below the threshold and window energy ($E+\Delta E$) can be counted using the window operation thereby rejecting the unwanted, low/high energy pulses.

2.6.1.6. Data acquisition system. The data acquisition system (PARA ELECTRONICS, Mumbai, India) employs an Intel 8085 microprocessor based system for controlling its operation. The interactive LCD display enables the user to set the dwell time, number of events, baud rate and other printing parameters with a compatible RS-232 output. The counters in the data acquisition system are configured around two Intel 8253 timer/counter integrated circuits. This clock is used as the reference in the dwell time setting. The important constituent in the data acquisition system is software that enables users to select the parameters, acquire the data and control the printing operation.

3. Tomography system design

In the present investigation, the test section was a perspex cylindrical bubble column of 385 mm internal diameter, 3.2 m height and 6 mm thickness. A schematic diagram is shown in Fig. 3. Sieve plate spargers were placed between the column and distributor chamber having a drain at the bottom and a gas inlet at the side. The material of the test section has a density almost equal to the water and attenuation through it is not so great so as to allow the measurement of the radiation at the detector. Transmission is very low at the centre and it increases at the wall. This is due to the decrease of the path length near the wall region of the test section. For the design highest transmission value was taken. For the obvious reasons of having the highest emission ratio and also highest half-life, the ^{137}Cs source was used in the present investigation as described earlier. Considering safety, the source was selected to be of low strength and also to have high sensitivity for the test section contents. Test section contents were water and water and air (two phase). The basis for the calculation of the source strength was taken 50 counts per second (disintegrations per second) through the test section contents near the wall (r/R=0.95). Since the counts are low, statistical errors may be large unless counting is over large times. A counting time of 60 s was selected which gives reasonably good number of counts through the test section. For the average transmission of 0.325 (0.15 and 0.5 at the centre and near wall, respectively), the sensitivity is 1.02, which means there will be less error in counting of the photons in two-phase, as they are highly sensitive to the water. For the given experimental conditions, the source strength Ac in Curie was found to be 55.5 μCi. A source having strength of 67.5 μCi was used in the present investigation.

The detectors used in the present investigation are scintillation detectors having a NaI crystal activated with thallium. This inorganic crystal has 100% detecting efficiency with a relatively high decay constant. Higher decay constants are not favourable only when the count rate is higher than the 10^5 counts per second. So for the present work, these detector scintillators are ideal and the detectors are small in size so that, at any time, more number of detectors can be accommodated in an arc.

As discussed earlier the source was collimated to provide a fan beam subtending an angle sufficient to cover the entire radius of the column in the horizontal plane. Similarly detectors were collimated to arrest from the detection of low energy photons generated out of scattering effect during its transmission. The second term on the right-hand side of the Eq. (5) accounts for the effect of scattering of the gamma photons. Detectors were collimated in two different ways to study the effect of scattering on the measurement of radial hold-up profile in the bubble column. Initially, the detectors

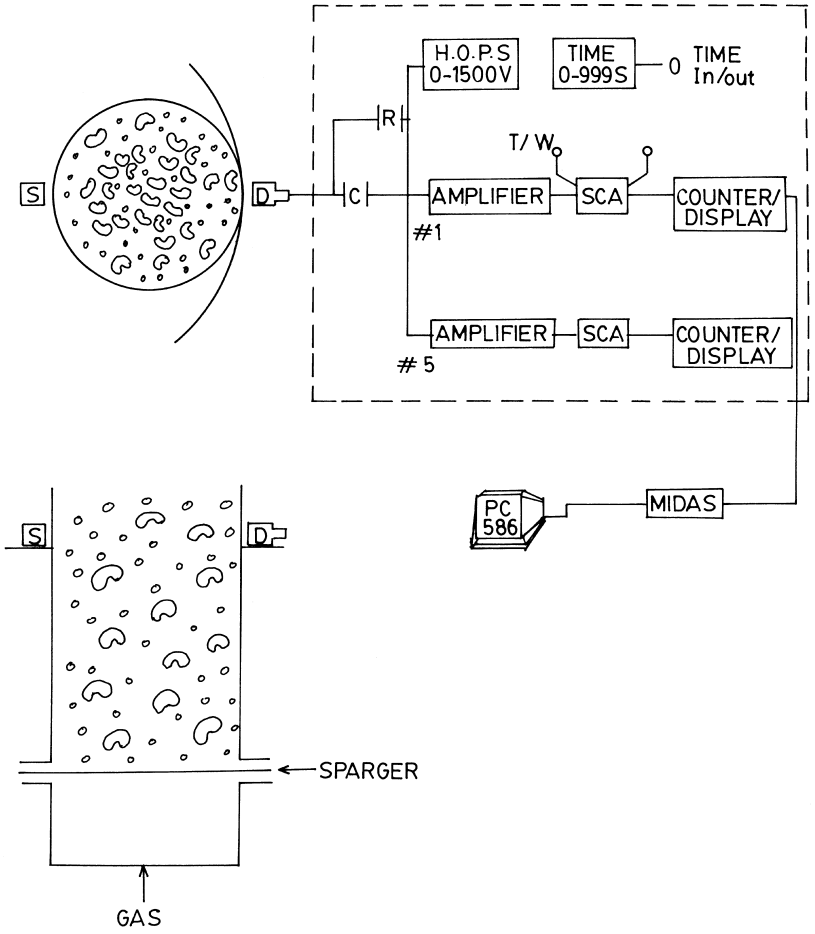

Fig. 3. Gamma ray tomography set-up; S: source; D: gamma ray detector; SCA: single channel analyzer; MIDAS: multi intelligent data acquisition system.

were collimated in lead brick with the entire front surface of the detector exposed for radiation detection (circular collimator). In this fashion, the detector detects the radiation beam with a diameter equal to the scintillator crystal diameter. Later the detectors were collimated in lead brick with a vertical slit of 6×18 and 30 mm thickness. So the resulting emerging beam from the source detected by the detector has the thickness of 6 mm, i.e. equal to the length of the vertical slit of the collimator. For the first case, the detector aperture D_d is equal to 2.54 cm and the X_d, the distance of the scattering event is minimum for our case is the length of chord passing through the r/R, normalized radius of 0.95. Then, the contribution of the second term to the scattering works out to be 0.0224 ($1-e^{-\mu t}$). For the later case, the term works out to be 0.00124 ($1-e^{-\mu t}$). So in the first case, the contribution of scattered photons is 18 times that of the second case, which is very significant. Consequently detectors collimated with a vertical slit of 6 mm×18 mm were used in the present investigation. These dimensions of the collimators are found to give least sample variance in the number of photons detected for a given dwell time of 60 s. The radial profiles of the two cases were shown in Fig. 4 for the same

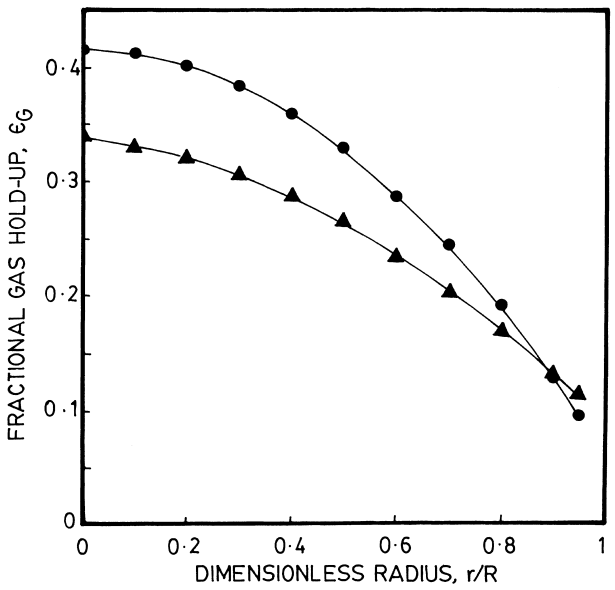

Fig. 4. Radial hold-up profiles with different collimator designs; V_G=0.24 m/s; H_D/D=5; d_O=1 mm; (▲): circular collimator; (●) vertical slit collimator.

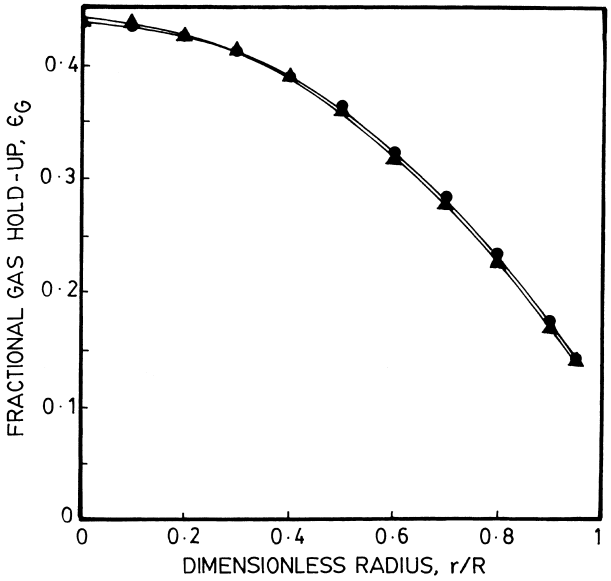

Fig. 5. Reproducibility of the technique; (●): trial 1; (▲): trial 2; V_G=0.24 m/s; H_D/D=5.

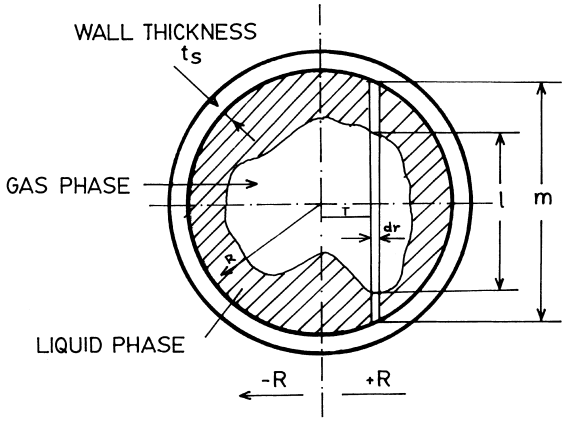

Fig. 6. Schematic of radiation absorption technique.

experimental conditions. The integrity of these profiles was checked with comparison of the cross-sectional average with column average hold-up estimated from the measurement of bed expansion. The cross sectional average of the column was calculated using the following expression.

$$\bar{\varepsilon}_G = \frac{1}{\pi R^2}\int_0^R 2\pi\varepsilon(r) r \mathrm{d}r \tag{6}$$

For the circular collimators the cross sectional average hold-up is 0.205 and for vertical slit collimator it is 0.241 which is in agreement with the column average hold-up of 0.243. The reproducibility of the technique was found to be 98% and it is shown in Fig. 5.

4. Measurements and estimation of hold-up profile

The basic principle behind the measurement of radial profile is based on the detection of attenuated gamma ray photons (Pike et al. [15]). The attenuation of monoenergetic beam passing through a thin homogeneous absorbing medium of uniform thickness is given by

$$I = I_O e^{-\mu t} \tag{7}$$

where I_O and I are the intensities of the incident and emerging beams respectively, μ the linear absorption coefficient and t the thickness of the absorbing medium.

The attenuation of the beam through a tube full of gas and liquid and with two-phase flow is given by the following expressions (see Fig. 6):

$$I_G = I_O e^{-(\mu_S 2t_s + \mu_G m)} \tag{8}$$

$$I_L = I_O e^{-(\mu_S 2t_s + \mu_L m)} \tag{9}$$

$$I_{TP} = I_O e^{-(\mu_S 2t_s + \mu_G L + \mu_L (m-L))} \tag{10}$$

From the above expressions, equation for the local chordal hold-up can be derived as

$$\varepsilon_{Chord} = \frac{\ln(I_{TP}/I_L)}{\ln(I_G/I_L)} \tag{11}$$

where I_{TP}, I_G and I_L are the intensities of the gamma rays in two phase, only gas and liquid phases, respectively.

The 11 chordal hold-ups were measured in the bubble column passing through the normalized radius, r/R of 0 to 0.95. The respective chordal lengths for the bubble column are 385, 382.2, 376.5, 366.1, 351.7, 333.4, 307.4, 276, 230.6, 167.5, and 120.2 mm. Experiments were carried out in heterogeneous regime (V_G>0.05 m/s) and for five superficial gas velocities of 0.063, 0.12, 0.18, 0.24 and 0.29 m/s. The concept of radial symmetry has been well established in bubble columns as also observed by Kumar et al. [16,17], Shollenberger et al. [18], Bukur et al. [10], Yao et al. [19], Yu and Kim [20] and Hills [21], so only half of the column was scanned.

The experimental methodology adopted for the chordal hold-up measurements was partly fan beam scanning and partly pencil beam scanning. The detectors were moved in an arc equal to the outer diameter of column with angles equal to the 0, 6, 12, 18, 24, 30, 37.5 and 44.5° from the axis of the source as shown in Fig. 7A. These angles cut the diameter at the r/R positions of 0, 0.1, 0.2, 0.3, 0.4, 0.5, 0.6 and 0.7, respectively. After this normalized radial position of 0.7, the pencil beam scanning was done at r/R locations of 0.8, 0.9 and 0.95. In compton scattering, the incoming gamma ray photon deflects through an angle with respect to its original direction. This process leads to the partial or complete transfer of the gamma ray photon energy to electron energy. This results in sudden and abrupt changes in gamma ray photons existence, which either disappear completely or scatter through a large average angles as low

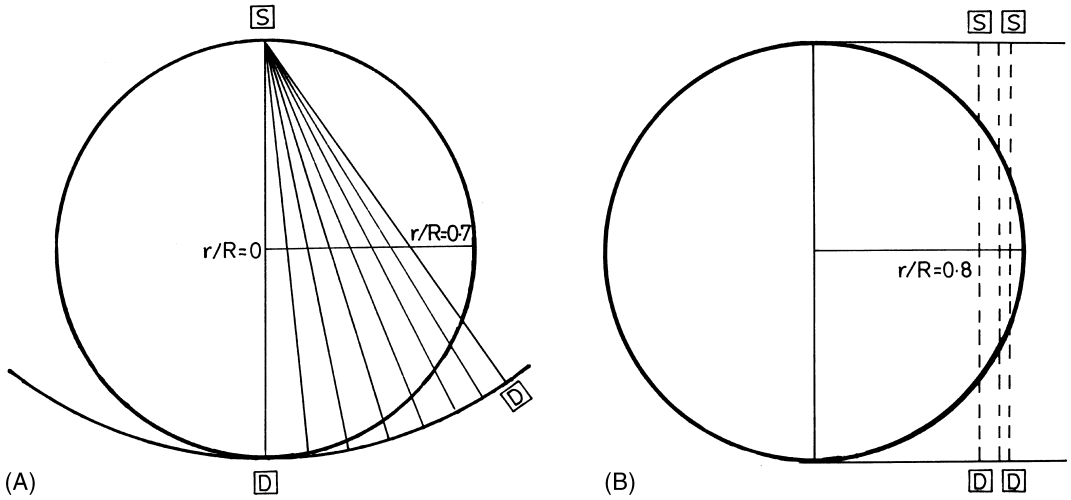

Fig. 7. (A) Schematic of fan beam scanning; (B) schematic of pencil beam scanning.

energy photons. As the path length through the medium between source and detector is less in the near wall region, there is possibility to detect the low energy scattered photons by detectors. For fan beam scanning, counted photons due to scattering comprised 5% of the total counted photons and this can increase (up to 50%) as the path length between source and detector decreases, resulting in the introduction of more error [22]. So for this reason, a pencil-beam scanning was adopted after the r/R (normalized radius) of 0.7 as shown in Fig. 7B. During fan beam scanning, the source was kept fixed at the centre of column and detectors were moved in an arc of radius 39 cm. And during pencil-beam scanning, both the source and the detector were moved simultaneously in parallel to the diameter.

The radial hold-up profiles were estimated using chordal hold-ups by Abel's inversion formula. This technique is based on a simple formula. Chordal hold-ups are fitting to a polynomial of even powers and then the radial hold-up profile is also polynomial of the same even powers (Vest [23] and Shollenberger et al. [18]).

The intensity of a monoenergetic radiation beam 'I', measured when the beam passes through a length of attenuating medium of 't', the transmission is given by Beer–Lambert's law, expressed as

$$T = \frac{I}{I_O} = \exp(-\mu t) \tag{12}$$

I_O is the incident radiation intensity, μ the attenuation coefficient. The attenuation is given by

$$A = -\ln\left(\frac{I}{I_O}\right) = \mu t \tag{13}$$

Attenuation coefficient can be reconstructed if the spatial variation of the attenuation is known as both of them are linearly related.

Reconstruction has been done using the Abel inversion described by Shollenberger et al. [18]. If $f(r, R)$ is a function of radial position within a circle of radius R, then its Abel transform is

$$\varphi(x, R) = 2\int_x^R \frac{f(r, R)r}{\sqrt{r^2 - x^2}}\mathrm{d}r \tag{14}$$

which is a line integral along the projection in y direction at x. On inversion of the above formula for $f(r, R)$ in terms of φ using the Abel inversion formula

$$f(r, R) = -\frac{1}{\pi}\int_r^R \frac{(\mathrm{d}\varphi/\mathrm{d}x)}{\sqrt{x^2 - r^2}}\mathrm{d}x \tag{15}$$

The projection (chord) is just a line integral of f, given by

$$\psi(x, R) = \frac{\varphi(x, R)}{2\sqrt{R^2 - x^2}} \tag{16}$$

which is a line integral of f along the ray at x divided by the path length. Both the function f and ψ interrelated and one is an even polynomial and other is also as even polynomial of the same degree. Expressions for f and ψ are given by

$$f(r, R) = \sum_{m=0}^{N} a_m \left(\frac{r}{R}\right)^{2m} \tag{17A}$$

$$\psi(x, R) = \sum_{n=0}^{N} b_n \left(\frac{x}{R}\right)^{2n} \tag{17B}$$

Shollenberger et al. [18] derived the reconstruction relations as

$$a_m = \sum_{n=0}^{N} C_{mn} b_n \tag{18A}$$

$$b_n = \sum_{m=0}^{N} d_{nm} a_m \tag{18B}$$

where

$$C_{mn} = \begin{cases} -\left[\dfrac{2m+1}{2^{2n}(2n-2m-1)}\right]\binom{2n-2m}{n-m}\binom{2m}{m}, & m \le n \\ 0, & m > n \end{cases} \tag{19}$$

$$d_{nm} = \begin{cases} -\left[\dfrac{2^{2n}}{(2m+1)}\right]\dfrac{\binom{2n-2m}{n-m}}{\binom{2m}{m}}, & n \le m \\ 0, & n > m \end{cases} \tag{20}$$

Radial symmetrical hold-up profile reconstruction was done as follows: (i) measure the chordal hold-ups at different x locations; (ii) fit the chordal projections with even powers of r/R to find out b_n; (iii) calculate C_{mn} to determine a_m and the radial profile. The second-order and fourth-order polynomial with even powers of r/R locations was used to fit the chordal hold-ups. A fourth-order polynomial was found to be optimal and it was used for all the calculations.

Fig. 8 shows the typical radial hold-up profiles of the bubble column measured at height to diameter ratio of five with superficial gas velocity as parameter for the sieve plate sparger with 1 mm diameter holes. Extensive experimental results based on this technique can be found in Parasu Veera and Joshi [24,25].

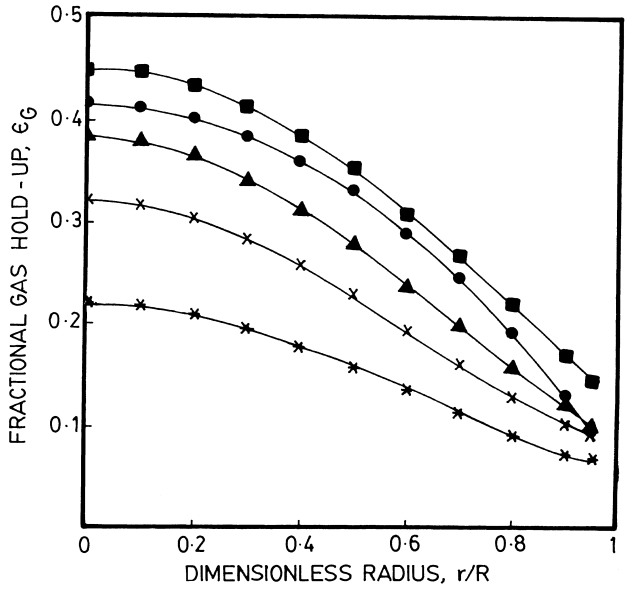

Fig. 8. Typical radial hold-up profiles; H_D/D=5; d_O=1 mm; (■): V_G=0.29 m/s; (●): V_G=0.24 m/s; (▲): V_G=0.18 m/s; (×): V_G=0.12 m/s; (⋆): V_G=0.06 m/s.

5. Conclusions

Gamma ray tomography scanning technique has been successfully employed for the measurement of radial hold-up profiles in a bubble column reactor. The systematic and simple design procedure of the tomography system has been discussed for air–water system. Both fan-beam (r/R=0 to 0.7) and pencil-beam (r/R=0.8 to 0.95) scanning was employed for the measurement of hold-up profiles. Scattering effect near the column wall region is reduced significantly by employing the pencil-beam scanning. Further, collimator design and dwell time was optimised for the given experimental conditions. Using this knowledge, tomography scanning system can be designed and used for the industrial columns. This technique will be useful as a diagnostic tool for solving the flow pattern problems for laboratory and as well industrial scale reactors.

Acknowledgements

Acknowledgements are due to Prof. J.B. Joshi for his help and encouragement in the present work. The author also acknowledges University Grants Commission, Government of India, for the award of fellowship.

References

[1] L.G. Neal, S.G. Bankoff, AIChE J. 9 (1963) 490.
[2] J.B. Joshi, U. Parasu Veera, Ch.V. Prasad, D.V. Phani Kumar, N.S. Deshpande, S.S. Thakre, B.N. Thorat, Gas hold-up structure in bubble column reactors, in: Proceedings of Indian National Science Academy, PINSA, 64(4), (1998) 441.
[3] J.M. Begovich, J.S. Watson, AIChE J. 24 (1978) 351.
[4] S.K. Achwal, J.B. Stepanek, Chem. Eng. Sci. 30 (1975) 1443.
[5] J.M.R. Delhaye, R. Semeria, J.C. Flamand, J. Heat Transfer 95 (1973) 365.
[6] M.A. Bennet, R.M. West, S.P. Luke, X. Jia, R.A. Williams, Chem. Eng. Sci. 54 (1999) 5003.
[7] M. Wang, A. Dorward, D. Vlaev, R. Mann, Chem. Eng. J. 77 (2000) 93.
[8] L. Xu, Y. Han, L-A. Xu, J. Yang, Chem. Eng. Sci. 52 (1997) 2171.
[9] W. Weigand, B.S. Hoyle, IEEE Trans. Ultra Ferroelec. Frequ. Control UFFC 36 (1989) 652.
[10] W. Li, B.S. Hoyle, Chem. Eng. Sci. 52 (1997) 2161.
[11] D.B. Bukur, J.G. Dalay, S.A. Patel, Ind. Eng. Chem. Res. 35 (1996) 70.
[12] A.C.M. Chan, S. Benerjee, Nucl. Instrum. Methods 190 (1981) 135.
[13] W.L. Swift, F.X. Dolan, P.W. Runstadler, Measurements in polyphase flows, in: Proceedings of the Winter Annual Meeting of ASME, San Fracisco, 1978, p. 25.
[14] A.S. Khare, Development of radio active tracer techniques and its application to the design of multiphase reactors, Ph.D. Thesis, University of Mumbai, 1989.
[15] R.W. Pike, B. Wilkins Jr., H.C. Wards, AIChE J. 11 (5) (1965) 794.
[16] S.B. Kumar, D. Moslemain, M.P. Dudukovic, Flow Meas. Instrum. 6 (1995) 61.
[17] S.B. Kumar, D. Moslemain, M.P. Dudukovic, AIChE J. 43 (1997) 1414.

[18] K.A. Shollenberger, J.R. Torczyski, D.R. Adkins, T.J. O'Herns, N.B. Jackson, Chem. Eng. Sci. 52 (1997) 2037.
[19] B.P. Yao, C. Zheng, H.E. Gasche, H. Hofmann, Chem. Eng. Process 29 (1991) 65.
[20] Y.H. Yu, S.D. Kim, Chem. Eng. Sci. 46 (1991) 313.
[21] J.H. Hills, Trans. I. Chem. E 52 (1974) 1.
[22] Hermann, Image Reconstruction From Projection: The Fundamental of Computerized Tomography, Academic Press, New York, 1980.
[23] C.M. Vest, Appl. Optics 24 (23) (1985) 4089.
[24] U. Parasu Veera, J.B. Joshi, Trans. I. Chem. E. 77 (1999) 303.
[25] U. Parasu Veera, J.B. Joshi, Trans. I. Chem. E. 78 (2000) 425.